Brain Imaging and Behavior (2017) 11:640–648
DOI 10.1007/s11682-016-9541-6

ORIGINAL RESEARCH

Methylene blue modulates functional connectivity in the human brain

Pavel Rodriguez[1,2] · **Amar P. Singh**[2] · **Kristen E. Malloy**[1] · **Wei Zhou**[1] · **Douglas W. Barrett**[3] · **Crystal G. Franklin**[1] · **Wilson B. Altmeyer**[2] · **Juan E. Gutierrez**[2] · **Jinqi Li**[1] · **Betty L. Heyl**[1] · **Jack L. Lancaster**[1] · **F. Gonzalez-Lima**[3] · **Timothy Q. Duong**[1]

Published online: 10 March 2016

Abstract Methylene blue USP (MB) is a FDA-grandfathered drug used in clinics to treat methemoglobinemia, carbon monoxide poisoning and cyanide poisoning that has been shown to increase fMRI evoked blood oxygenation level dependent (BOLD) response in rodents. Low dose MB also has memory enhancing effect in rodents and humans. However, the neural correlates of the effects of MB in the human brain are unknown. We tested the hypothesis that a single low oral dose of MB modulates the functional connectivity of neural networks in healthy adults. Task-based and task-free fMRI were performed before and one hour after MB or placebo administration utilizing a randomized, double-blinded, placebo-controlled design. MB administration was associated with a reduction in cerebral blood flow in a task-related network during a visuomotor task, and with stronger resting-state functional connectivity in multiple regions linking perception and memory functions. These findings demonstrate for the first time that low-dose MB can modulate task-related and resting-state neural networks in the human brain. These neuroimaging findings support further investigations in healthy and disease populations.

Keywords Multimodal fMRI · Methylene blue · Evoked response · Functional connectivity · Default mode network

Introduction

Methylene blue (MB) is a FDA-grandfathered drug currently used to treat carbon monoxide, methemoglobinemia and cyanide poisoning in humans (Scheindlin 2008; Clifton and Leikin 2003). At a low dose (1–4 mg/kg), MB can cross the blood-brain barrier and form a reversible reduction-oxidation system with auto-oxidizing capacity (Bruchey and Gonzalez-Lima 2008). MB has redox recycling properties in that it acts as a renewable electron cycler and facilitates electron transfer in the mitochondrial electron transport chain by accepting electrons from NADH and transferring them to cytochrome c oxidase, bypassing complexes I-III (Clifton and Leikin 2003; Scott and Hunter 1966). This translates to more energy and decreased free radical toxicity for the cell. Low-dose MB increased brain glucose uptake, oxygen consumption and evoked fMRI responses in the rat brain under normal and hypoxic conditions in vivo (Lin et al. 2012; Huang et al. 2013). MB also has a long history of safe usage. Its pharmacokinetics, side effect profile, and contraindications of low-dose MB are well-known, and importantly, minimal in humans (Peter et al. 2000; Walter-Sack et al. 2009).

Low-dose MB has recently been shown to reduce neurobehavioral impairment in animal models of optic neuropathy (Zhang et al. 2006), Parkinson's disease (Rojas et al. 2012), and Alzheimer's disease (Callaway et al. 2002), and to reduce functional deficit and MRI lesion volume in rodent models of ischemic stroke (Shen et al. 2013; Rodriguez et al. 2014),

Electronic supplementary material The online version of this article (doi:10.1007/s11682-016-9541-6) contains supplementary material, which is available to authorized users.

✉ Pavel Rodriguez
rodriguezp3@uthscsa.edu

✉ Timothy Q. Duong
duongt@uthscsa.edu

[1] Research Imaging Institute, The University of Texas Health Science Center at San Antonio, 8403 Floyd Curl Drive, San Antonio, TX 78229-3900, USA

[2] Department of Radiology, The University of Texas Health Science Center at San Antonio, 7703 Floyd Curl Drive, Mail Stop 7800, San Antonio, TX 78229, USA

[3] Department of Psychology and Institute for Neuroscience, The University of Texas at Austin, Austin, TX 78712, USA

traumatic brain injury (Watts et al. 2015; Watts et al. 2014), and fear extinction memory (Gonzalez-Lima and Bruchey 2004). Low-dose MB also has memory-enhancing effects, first described more than 30 years ago in animals (Martinez et al. 1978) and confirmed more recently in rodents (Rojas et al. 2012; Wrubel et al. 2007) and humans (Telch et al. 2014).

MB also prevented memory impairment in rats with local inhibition of mitochondrial respiration in the posterior cingulate cortex by maintaining cingulo-thalamo-hippocampal effective connectivity (Riha et al. 2011). The redox chemistry of MB may also facilitate other cellular processes that extend beyond the mitochondria (Bruchey and Gonzalez-Lima 2008; Jiang et al. 2015). Although there are many preclinical studies of MB, the neural correlates of MB in the human brain are unknown.

We report the first neuroimaging study to evaluate the effects of low-dose MB on the functional connectivity of the human brain, in a randomized double-blinded, placebo-controlled clinical trial in healthy adults using task-based and task-free functional MRI (fMRI). MRI was used to evaluate the effects of MB on cerebral blood flow (CBF) during a visuomotor task, and resting functional connectivity and cerebrovascular reactivity. Based on prior animal studies, we tested the hypothesis that MB will modulate the evoked neural response and resting-state neural networks.

Methods

Study design

We received approval by the Institutional Review Board of the University of Texas Health Science Center at San Antonio to conduct a double-blinded, placebo-controlled prospective trial. Twenty-eight participants were enrolled between September 2013 and December 2014, and randomized to 280 mg of oral USP grade methylene blue (methylthioninium chloride, PCCA, Houston, Texas) or placebo (FD&C Blue #2) after completing baseline fMRI tasks. Subjects were asked to abstain from caffeine and to eat a very light meal the morning of the MRI scan visit. The 280 mg dose selection was estimated as a 4 mg/kg dose (for an average 70 kg body weight) because the hormetic property of MB has mitochondrial enhancing effects at the low-dose range of 0.5–4 mg/kg, and opposite negative effects at doses >10 mg/kg (Bruchey and Gonzalez-Lima 2008). The fMRI tasks were simulated with the subjects prior to entering the scanner. A second set of identical MRI data from baseline was acquired 60 min after MB or placebo administration to allow for peak venous drug absorption (Peter et al. 2000). All subjects were scanned using the same paradigm order and scanner (Fig. 1). The study participants and investigators remained blinded until the conclusion of the analysis.

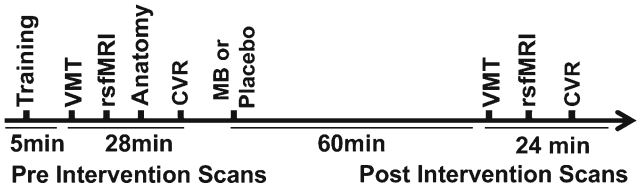

Fig. 1 Schematic overview of fMRI scans and surveys

Eligibility criteria

Inclusion: English-speaking, healthy subjects between the ages 18–65 years old. Only 4 subjects were older than 40 and were evenly divided between groups. Exclusion criteria included neurological, psychiatric (claustrophobia, psychotic or panic disorders), cardiovascular (hypertension, diabetes), hepatic or renal disorders (including prior transplants), hypersensitivity to MB or thiazide diuretics/phenothiazines, glucose-6-phosphate dehydrate deficiency (G6PD), contraindication to MRI, pregnancy or currently breastfeeding, colorblindness, methemoglobinemia, taking any psychiatric or serotonergic medication (currently or within the last 5 weeks), gastric bypass or any other surgery that could interfere with normal drug absorption.

Experimental tasks

Stimuli were presented via an LCD projector, which was visible to the subject by a mirror mounted to the head coil and a camera was used to monitor subject safety and compliance. *Visuomotor task* (*VMT*): The subject was instructed to tap fingers vigorously when a circular (Fig 2b), reversing black-and-white flickering checkerboard pattern appeared on the screen, and to remain still when a fixation cross was shown. The VMT consisted of 6 alternating epochs of rest with 5 epochs of tapping that each lasted 45 s. *Resting functional connectivity task* (*rsfMRI*): The subject was instructed to close eyes, not to think about a particular topic and to not fall asleep. *Cerebrovascular reactivity* (*CVR*): The subject was moved out of the scanner to put on a non-rebreather mask at the end. Pre and post intervention 5 % carbon dioxide in air for 5 min was administered to evaluate the effects of MB on vasodilation. The paradigm was 1 min room air and 5 min of 5 % CO_2.

Image acquisition

MRI studies were performed using the same Siemens TIM Trio 3.0 Tesla scanner using a 12-channel head-coil.

A standard 3D MPRAGE anatomical T1-weighted MRI at 1 × 1 × 1 mm resolution, 2.2 s repetition time, 2.8 ms echo time, 766 ms inversion time, 176 × 256 matrix, 208 slices, 13° flip angle was acquired at baseline for registration.

For rsfMRI studies, BOLD fMRI was acquired using a gradient echo-planar imaging sequence, 1.72 × 1.72 × 4.00 mm

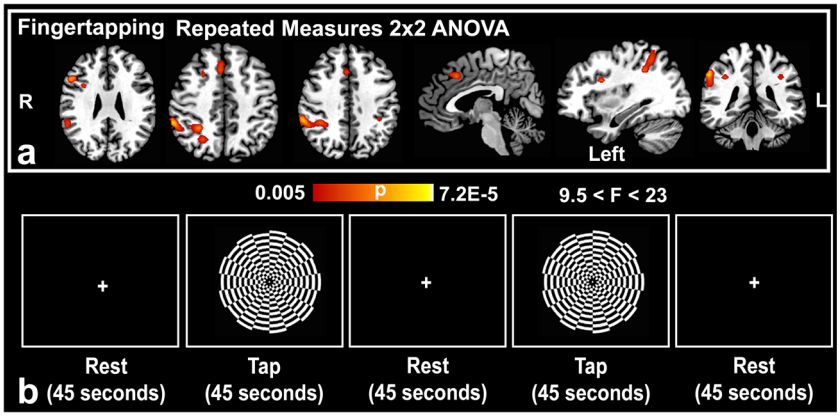

Fig. 2 (**a**) Repeated measures ANOVA results of the fingertapping phase of the visuomotor task (VMT) ($pFWE_{corrected} < 0.05$; $k > 10$ voxels; $N = 13$ per group, 24 degrees of freedom) reveals positive drug x time interactions in favor of an MB effect in the anterior cingulate cortex, and bilateral inferior parietal lobules (**b**) Representative block from the VMT composed of fingertapping and rest phases as demarcated by set times

voxel size, 2 s repetition time, and 30 ms echo time, 128 × 128 acquisition matrix, 220 × 220 mm field of view, 90° flip angle, parallel acceleration factor of 2, and 29 slices (4 mm thickness) without slice gap, 300 measurements (10 min).

For VMT and CVR studies, CBF was measured using a pseudo-continuous arterial-spin labeling sequence with echo-planar imaging, 3.44 × 3.44 × 4 mm voxel size, 4.5 s repetition time, 16 ms echo time, 64 × 64 acquisition matrix, 220 × 220 mm field of view, 90° flip angle, and 23 slices (4 mm thickness) without slice gap. For VMT and CVR, 121 and 80 tag-control pairs were acquired. The first measurement was discarded for the VMT.

Image analysis

VMT and CVR fMRI data from the VMT were realigned, coregistered to the structural volume, normalized to a standard Montreal Neurologic Institute (MNI) template, motion corrected and spatially smoothed (8-mm full width half maximum) using SPM8 (UCL). At the first level, CBF response changes for each condition (fingertapping or hypercapnia) were then estimated by fitting the time-course data with general linear model composed of box-car functions convolved with the canonical hemodynamic response function. Then, at the second-level using a random effects analysis, the first level-contrasts were used in a 2 × 2 repeated measures ANOVA using intervention (MB vs. Placebo) and time (Pre vs. Post) as factors to assess Drug x Time interactions (Gläscher and Gitelman 2008). This tested for between group effects and accounted for the change in the placebo group. The CBF response evoked in the visual, somatosensory and hypercapnic stimuli was tested using small volume analysis (cluster corrected pFWE < 0.05) with regions of interests generated from the WFU PickAtlas v 3.0 (Maldjian et al. 2003), nodes of the visuospatial network (intraparietal sulcus-frontal eye fields) (Geier et al. 2009; Shirer et al. 2012), and from meta-analysis of nodes of the default mode network (K. *C. fox* et al. 2015) and from visuomotor tasks (Witt et al. 2008). The directionality of the F contrasts was confirmed using SPM.

Maps of absolute mean cerebral blood flow were also generated for the VMT and CVR tasks using the ASL Data Processing toolbox (v. May 2012) (Wang et al. 2008). ASLtbx applies standard preprocessing and a validated CBF quantification model. The labeling efficiency = 0.8, blood-brain barrier partition coefficient = 0.9, blood T1 = 1.49 s and GM T1 = 1.4 s. Subject-space mean CBF maps were then coregistered to standard MNI template using affine FLIRT (FMRIB). Group level analysis of these processed mean CBF maps were then conducted using paired within group analysis. For this within-group analysis, z statistical parametric maps were cluster-corrected using z score of at least 2.3 and a whole-brain significance of at least $p < 0.05$. The same ROI's used in the above GLM analysis were also inspected. Two incomplete data sets were excluded from the MB group for the VMT and CVR.

Goodness of fit analysis The significant cluster results (F values converted to z-scores) of the VMT group 2 × 2 ANOVA analysis were compared against the published functional network templates generated at rest by the Stanford Functional Imaging in Neuropsychiatric Disorders lab (http://findlab.stanford.edu/functional_ROIs.html)(Shirer et al. 2012). The mean z-score of all the voxels outside the published network template ($z_{outside}$) were subtracted from the mean z-score of all the voxels from the proposed map that coincided with the published network template (z_{inside}) to calculate the GOF (i.e., $z_{inside} - z_{outside}$) as previously described (Lehmann et al. 2013; Greicius et al. 2007). Non-imaged infratentorial regions, or areas near the tentorium due to artifact, were excluded from the analysis. Our analysis included the 14 available individual functional templates from the FIND lab, and we included in the analysis GOF for every node in these networks. A previously published visuomotor task functional network template was not available for the analysis.

Resting state fMRI The drug effect on resting-state functional connectivity was assessed by detecting temporal correlation of the BOLD signals amongst different regions of the brain before and after MB or placebo administration. Functional connectivity analysis was performed using the CONN (v. 14) toolbox (Whitfield-Gabrieli and Nieto-Castanon 2012). Preprocessing using SPM and CONN included realignment and unwarping, structural segmentation and normalization, functional normalization, functional outlier detection (ART-based scrubbing), and spatial smoothing (8-mm full width half maximum). Principal components using segmented white matter, cerebral spinal fluid and motion realignment parameters were used as confounds without a need for global signal regression using the CompCor method (Whitfield-Gabrieli and Nieto-Castanon 2012). Data were temporally band-pass filtered to 0.008 Hz-0.09 Hz. Linear detrending and despiking after regression was also applied. A weighted GLM functional connectivity analysis using a hemodynamic response function weighting and bivariate correlation was used for seed to voxel first level analysis. Signal was extracted from a set of 10-mm spherical voxels of interest (VOI's) centered on 132 regions in the Automated Anatomical Labeling (AAL) atlas (Tzourio-Mazoyer et al. 2002; Pamplona et al. 2015), which is a macroanatomical parcellation of the single subject MNI-space template brain. Spherical seeds were also generated using nodes of the default mode network (Whitfield-Gabrieli and Nieto-Castanon 2012) and fronto-parietal attention network (Markett et al. 2014). Fisher's Z-transformed correlations were computed. We applied an ANOVA analysis to test for (MB vs. placebo) x time (Pre vs. Post) interactions. Then, we performed post-hoc analysis of significant seeds with correlations ($z > 2.3$, $p = 0.01$) of these between-group and time differences (MB > Placebo and Post intervention > Pre Intervention) to isolate clusters that were covarying in same direction. Significant differences resulting from negative correlations were excluded. Results are reported at a voxelwise $p_{uncorrected} < 0.001$ and cluster-level threshold of $p < 0.05$ FDR corrected.

Results

The age, gender, years of education, positive and negative-affect-schedule (PANAS) scores (Table 1) and handedness did not differ between the MB and placebo groups ($p > 0.05$) using 2-sample t tests. Only subjects in the MB group reported transient urine coloration after leaving the imaging center.

VMT

The VMT produced no statistically significant differences in CBF between pre and post MB in the motor, somatosensory and visual cortex. However, MB intake was associated with significant drug (placebo vs. MB) x time (pre vs. post) interactions in the bilateral inferior parietal lobules, right inferior frontal gyrus (inferior operculum), right anterior cingulate gyrus, and right middle frontal gyrus (Fig 2a and Table 2). The directionality of these F contrasts was negative. The mean absolute CBF maps also confirmed significant decrease in CBF in these areas, but no change in the placebo (Fig 3a and b).

Table 1 Group characteristics

Characteristic	Placebo	MB
Age (yrs.) ± SD	30.6 ± 10.4	29.8 ± 9.7
Females/Males	8/5	10/5
Education (yrs.)	17.4	17.5
Right Handedness	80 %	85 %

Goodness of fit

Our observed suppressed VMT network was a task-related network that did not perfectly fit any of the 14 tested functional networks templates. A GOF was calculated for the nodes within these networks and we detected overlap between nodes of 8 out of the 14 networks (Table 3). The strongest fit was for the ventral DMN and for the visuospatial network, as indicated by each of these two networks showing overlaps with four regions of the VMT task-related network. But there was also some overlap to a lesser degree with regions in the precuneus, anterior/posterior salience, bilateral executive, and dorsal default mode networks. The region with the largest GOF score was the right inferior parietal lobule, Brodmann Area (BA) 40, which overlapped with the posterior salience network (3.1) and the right executive control network (3.0). The GOF was very poor for the basal ganglia, sensorimotor, auditory, higher visual, language, and primary visual networks, which had no overlap with the studied regions.

Cerebrovascular reactivity

Group analysis revealed no significant difference in cerebrovascular reactivity between the MB and placebo groups due to resting hypercapneic stimulus (data not shown).

Resting state fMRI

Multiple clusters ranging from 187 to 388 voxels were found with increased functional connectivity after MB intake relative to baseline (Table 4 and Table S1 with coordinates and post-hoc analysis correlations). There was increased functional connectivity between the left ventral intraparietal sulcus (a

Table 2 Brain regions displaying significant Drug x Time Interactions during the VMT after methylene blue relative to placebo

Region	Cluster	pFWE	F(1,24)*	Z*	X	Y	Z
Finger tapping							
Right inferior parietal lobule, precuneus	254	2.30E-04	26.96	4.05	60	−40	46
Right inferior frontal gyrus (operculum/ triangularis)	24	0.002	19.75	3.58	53	19	26
Right inferior frontal operculum	10	0.006	15.23	3.21	35	8	26
Right anterior cingulate gyrus	23	0.01	14.31	3.12	35	13	−6
Precuneus	19	0.02	12.29	2.91	46	8	2
Right middle frontal gyrus	19	0.01	14.23	3.11	−37	12	−6
Left inferior parietal lobule, postcentral gyrus	21	0.01	12.96	2.98	−37	−40	38

*The directionality of the F contrasts (and Z equivalent) was negative; $p_{uncorrected} < 0.005$, small volume cluster-corrected pFWE <0.05, MNI, k = No. of voxels (1.719 × 1.719 × 4 mm^3 per voxel), $N = 13$ per group, 24 degrees of freedom

node within the fronto-parietal attention network), and the right intracalcarine cortex and lingual gyrus (pFDR =0.0003, 388 voxels). A seed in the posterior cingulate cortex showed increased functional connectivity with the left middle frontal gyrus, right insular cortex, and left precentral gyrus. The left frontal eyefield signal changes also correlated positively with the left precentral gyrus and the left middle frontal gyrus (pFDR =0.006) after MB intake. The right middle frontal gyrus had increased functional connectivity with the right middle temporal gyrus, and cerebellum Crus1. Finally, we detected strong increase in functional connectivity between the left hippocampus and the right cerebellum area 9 of the AAL atlas.

Discussion

This study used task-based and task-free fMRI to map the neural correlates of MB administration in humans. The major findings showed that low-dose MB: i) increased visual-motor task-induced deactivation of a task-related network and ii) increased functional connectivity amongst regions associated with working memory, visual and motor coordination. These findings suggest that MB can modulate neural networks after a single oral low dose.

We found no significant difference in stimulus-evoked CBF changes between the MB and placebo groups in the

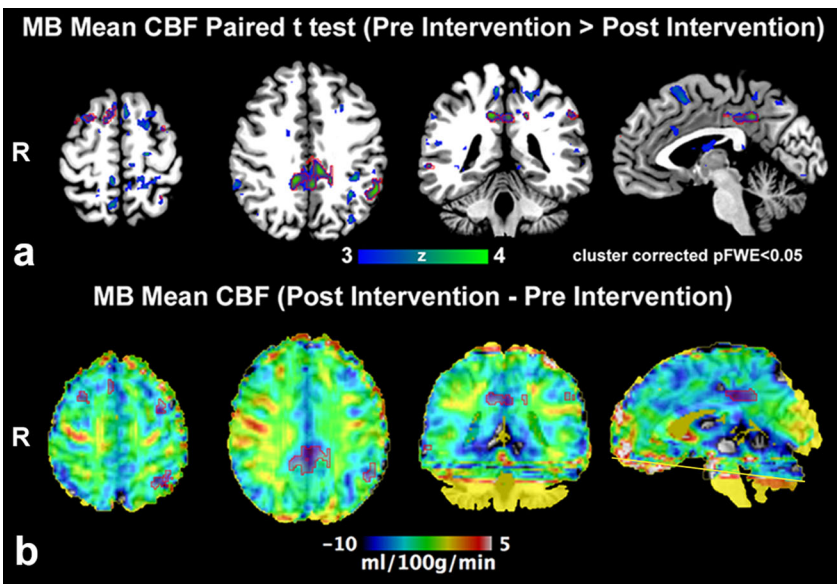

Fig. 3 (**a**) Paired analysis (Pre intervention > Post Intervention) of absolute mean CBF (pCASL fMRI) demonstrates larger clusters prior to methylene blue (MB) administration ($n = 13$); significant clusters are outlined by red ROI. (**b**) Post intervention minus Pre intervention group absolute mean CBF average demonstrates that the significant clusters belong to the posterior cingulate/precuneus, left inferior parietal lobule and prefrontal cortex consistent with a visuomotor network where CBF is greater prior to MB intervention. Mild CBF increase in the right motor cortex did not achieve significance. Artifact limits evaluation adjacent to the inferior imaging plane (yellow line)

Table 3 Goodness of Fit analysis of nodes in our observed network with previously described functional brain networks

Network	Location of Node	GOF
Anterior salience	Anterior Cingulate	2.4
Dorsal DMN	Posterior Cingulate	1.9
Left executive control	Left inferior parietal lobe	2.4
Posterior salience	Left inferior parietal lobe supramarginal gyrus, BA 40	2.2
	Posterior cingulate, BA 31	2.0
	Right inferior parietal lobe, BA 40	3.1
Precuneus	Precuneus, cuneus, BA 7/19	2.0
	Left inferior parietal lobe, angular gyrus	2.1
	Right inferior parietal Lobe, angular gyrus, BA 39	2.4
Right executive control	Medial frontal gyrus, BA 8	2.2
	Right inferior parietal lobe, BA40	3.0
Ventral DMN	Cuneus, BA 19	1.7
	Precuneus, BA 7	2.2
	Right superior frontal gyrus, BA 6	2.1
	Superior occipital gyrus, BA 19	2.2
Visuospatial	Precuneus, left superior and inferior parietal lobe, BA40	2.2
	Left inferior frontal gyrus, BA9	2.0
	Right precuneus, right superior and inferior parietal lobe, BA7	2.9
	Right inferior frontal gyrus, BA9	2.5

Goodness of Fit (GOF) = z_{inside} - $z_{outside}$; a larger GOF indicates a better fit

motor, somatosensory and occipital cortex. However, we found a significant decrease in CBF after MB intake in clusters located in the posterior cingulate cortex, prefrontal cortex and inferior parietal lobes associated with the VMT. These clusters overlap mostly with nodes within the visuospatial network, a network that involves frontal and intraparietal sulcus regions, which have been implicated in spatial working memory, and the ventral DMN, a network of functionally connected cortical regions that are active at "rest", but are deactivated by cognitive processes (M. D. Fox et al. 2005; Raichle 2015).

Interestingly, other neuroenhancing drugs that work by different mechanisms than MB have also been associated with promoting task-induced deactivation of a neural network, including mainly regions of the DMN, which is normally more active at rest. For example, modafinil, a norepinephrine and dopamine transporter inhibitor, which is used to treat narcolepsy and excessive daytime sleepiness disorders, was shown to suppress the DMN using a visual-motor task(Minzenberg et al. 2011). Similar to our VMT, the investigators asked participants to repeatedly press a button as fast as possible. Contrary to MB's lack of effect on reaction time, modafinil

Table 4 Brain regions with significant increases in FC relative to baseline and change in placebo (Methylene Blue > Placebo and Post Intervention > Pre Intervention)

Source Seed (location)	Target	pFDR	k	z'	t
Left ventral intraparietal sulcus	Right intracalcarine cortex, right lingual gyrus	0.0003	388	0.26	5.11
Posterior cingulate, precuneus	Right insular cortex	0.003	265	0.22	7.72
Left frontal eyefield	Left precentral gyrus, left middle frontal gyrus	0.006	254	0.25	4.92
Left temporal pole	Left superior frontal gyrus, left paracingulate gyrus	0.008	258	0.25	5.7
Left intracalcarine cortex	Lateral occipital cortex superior division	0.022	189	0.29	4.85
Left hippocampus	Cerebellum 9 right	0.025	187	0.2	7.04
Right middle frontal gyrus	Right inferior temporal gyrus (temporooccipital), temporal occipital fusiform cortex, right middle temporal gyrus (temporooccipital part), cerebellum crus1	0.031	209	0.24	5.47
Right temporal pole	Left superior frontal gyrus, left paracingulate gyrus	0.037	187	0.26	4.72

Cluster corrected pFDR <0.05, k = no. of voxels (1.719 × 1.719 × 4 mm^3 per voxel), z' = Fisher corrected correlation, 26 degrees of freedom, N = 15 MB and N = 13 Placebo, detailed results in Table S1

facilitated sensorimotor processing speed. The dopaminergic stimulant methylphenidate, used to treat attention deficit hyperactivity disorder, was also shown to suppress activity of the DMN network using an inhibitory control task (Liddle et al. 2011). During the paced Go/No-go task, children treated with methylphenidate participated more in the task, and this was reflected by greater DMN deactivation. Our data indicate that MB, like other neuroenhancing drugs, is associated with promoting task-induced deactivation of the DMN.

Our results suggest that the VMT task led to greater suppression of regions in the visuospatial network and the ventral DMN after MB relative to placebo, which may mean increased activity within these regions prior to initiation of the task. The findings that cognitive enhancers with very different biochemical mechanisms all promote deactivation of the DMN suggest that this brain phenomenon is not readily explainable at a biochemical level. One potential higher-order explanation may be related to the interactive network organization of the brain (McIntosh and Gonzalez-Lima 1995; M. D. Fox et al. 2005). Our fMRI findings with MB are consistent with this interpretation of network interactions in the brain (McIntosh 2000).

MB increased resting-state functional connectivity between cortical areas responsible for directing visuomotor coordination, such as the intraparietal sulcus and the intracalcarine cortex/lingual gyrus. Functional connectivity increased within cortical areas important for vision such as the occipital and intracalcarine cortices. There was also a significant increase between the frontal eye field and the prefrontal and motor cortex. MB treatment was also associated with increased functional connectivity between the anterior temporal pole and the left superior frontal and left paracingulate gyrus. The anterior temporal pole has been shown to encode abstract conceptual properties of objects and this is theorized to be important for a framework linking perception and memory (Jeneson and Squire 2012; Pankevich et al. 2014). We also detected a strong increase in functional connectivity between the left hippocampus and the right cerebellum area 9. These findings are in general agreement with those from the VMT tasks, further supporting the notion that MB modulates resting-state networks related to visuomotor coordination and networks linking perception and memory functions.

Group analysis revealed no significant difference in cerebrovascular reactivity in the activated areas associated with VMT. These findings are consistent with an animal fMRI study using 5 % CO2 inhalation that showed that low-dose MB does not affect cerebrovascular reactivity in rats (Huang et al. 2013). These findings indicate that low-dose MB does not exert an observable effect on vascular reactivity in the brain. On the other hand, low-dose MB increases the brain oxygen consumption, as measured in vitro and in vivo in animal models (Rojas et al. 2012; Huang et al. 2013). Therefore, the task-based fMRI signals modified by MB administration may be more likely attributed to changes in tissue oxygen consumption rather than changes in basal CBF or vascular tone.

Our exploratory, proof-of-concept, fMRI study has several limitations. Although we relied on a small sample size, this is not unusual in multimodal fMRI studies given the high statistical power and sensitivity of the techniques. Additional studies are needed to test the results in larger sample sizes. We primarily wanted to reproduce the evoked fMRI response in humans, which was previously tested in rodents using a single dose (Huang et al. 2013). We did not measure the concentration of MB in the blood, but a prior pharmaceutical study using oral dosage showed that the drug reached its maximum concentration in whole blood one hour after oral MB administration in healthy subjects (Peter et al. 2000). It is important to note that the previous MB concentration was higher in rodents than in humans due to differences in administration (oral vs. intravenous). Additional chronic dosages will be tested in the future. We also attempted to test whether MB can broadly modulate resting state networks or sub-networks, and imposed strict thresholds on the correlation analysis to minimize the effects from noise. It is possible that we may have excluded some effects. The lack of behavioral scores for this study is also a limitation, but opens the door to other studies with larger sample sizes that are usually necessary to detect effects on behavioral measures.

Conclusion

Task-based and task-free fMRI in this randomized, double-blinded, placebo-controlled clinical study supported the hypothesis that a single low dose of MB modulates resting-state networks in the human brain. This suggests that MB enhances resting-state functional connectivity in brain regions associated with a visuomotor task and linking perception and memory functions, while promoting task-induced deactivation of regions that overlap mainly with ventral default mode and visuospatial networks. This work provides a neuroimaging foundation to pursue clinical trials of MB in healthy aging, cognitive impairment, dementia, and other conditions that might benefit from drug-induced neuroenhancement.

Acknowledgments The project was supported by support from the Julio C. Palmaz, MD, Endowment for Excellence in Radiology Research and by a Pilot Grant under the umbrella of the UL1TR001120 from the National Center for Advancing Translational Sciences (NCAT, NIH). The content is solely the responsibility of the authors and does not necessarily represent the official views of the NIH.

Compliance with ethical standards

Disclosures All authors report no competing interests.

Informed consent All procedures followed were in accordance with the ethical standards of the responsible committee on human

experimentation (institutional and national) and with the Helsinki Declaration of 1975, and the applicable revisions at the time of the investigation. Informed consent was obtained from all subjects for being included in the study.

References

Bruchey, A. K., & Gonzalez-Lima, F. (2008). Behavioral, physiological and biochemical hormetic responses to the autoxidizable dye methylene blue. *American Journal of Pharmacology and Toxicology*, *3*(1), 72–79. doi:10.3844/ajptsp.2008.72.79.

Callaway, N. L., Riha, P. D., Wrubel, K. M., McCollum, D., & Gonzalez-Lima, F. (2002). Methylene blue restores spatial memory retention impaired by an inhibitor of cytochrome oxidase in rats. *Neuroscience Letters*, *332*(2), 83–86. doi:10.1016/S0304-3940(02)00827-3.

Clifton 2nd, J., & Leikin, J. B. (2003). Methylene blue. *American Journal of Therapeutics*, *10*(4), 289–291. doi:10.1097/00045391-200307000-00009.

Fox, M. D., Snyder, A. Z., Vincent, J. L., Corbetta, M., Van Essen, D. C., & Raichle, M. E. (2005). The human brain is intrinsically organized into dynamic, anticorrelated functional networks. *Proceedings of the National Academy of Sciences of the United States of America*, *102*(27), 9673–9678. doi:10.1073/Pnas.0504136102.

Fox, K. C., Spreng, R. N., Ellamil, M., Andrews-Hanna, J. R., & Christoff, K. (2015). The wandering brain: meta-analysis of functional neuroimaging studies of mind-wandering and related spontaneous thought processes. *NeuroImage*, *111*, 611–621. doi:10.1016/j.neuroimage.2015.02.039.

Geier, C. F., Garver, K., Terwilliger, R., & Luna, B. (2009). Development of working memory maintenance. *Journal of Neurophysiology*, *101*(1), 84–99. doi:10.1152/jn.90562.2008.

Gläscher, J., & Gitelman, D. (2008). Contrast weights in flexible factorial design with multiple groups of subjects. < http://www.sbirc.ed.ac.uk/cyril/download/Contrast_Weighting_Glascher_Gitelman_2008.pdf> Accessed Feb. 2016.

Gonzalez-Lima, F., & Bruchey, A. K. (2004). Extinction memory improvement by the metabolic enhancer methylene blue. *Learning & Memory*, *11*(5), 633–640. doi:10.1101/lm.82404.

Greicius, M. D., Flores, B. H., Menon, V., Glover, G. H., Solvason, H. B., Kenna, H., et al. (2007). Resting-state functional connectivity in major depression: abnormally increased contributions from subgenual cingulate cortex and thalamus. *Biological Psychiatry*, *62*(5), 429–437. doi:10.1016/j.biopsych.2006.09.020.

Huang, S., Du, F., Shih, Y. Y., Shen, Q., Gonzalez-Lima, F., & Duong, T. Q. (2013). Methylene blue potentiates stimulus-evoked fMRI responses and cerebral oxygen consumption during normoxia and hypoxia. *NeuroImage*, *72*, 237–242. doi:10.1016/j.neuroimage.2013.01.027.

Jeneson, A., & Squire, L. R. (2012). Working memory, long-term memory, and medial temporal lobe function. *Learning & Memory*, *19*(1), 15–25. doi:10.1101/lm.024018.111.

Jiang, Z., Watts, L. T., Huang, S. L., Shen, Q., Rodriguez, P., Chen, C. H., et al. (2015). The Effects of Methylene Blue on Autophagy and Apoptosis in MRI-Defined Normal Tissue, Ischemic Penumbra and Ischemic Core. *PloS One*, *10*(6). doi:10.1371/journal.pone.0131929.

Lehmann, M., Madison, C. M., Ghosh, P. M., Seeley, W. W., Mormino, E., Greicius, M. D., et al. (2013). Intrinsic connectivity networks in healthy subjects explain clinical variability in Alzheimer's disease. *Proceedings of the National Academy of Sciences of the United States of America*, *110*(28), 11606–11611. doi:10.1073/pnas.1221536110.

Liddle, E. B., Hollis, C., Batty, M. J., Groom, M. J., Totman, J. J., Liotti, M., et al. (2011). Task-related default mode network modulation and inhibitory control in ADHD: effects of motivation and methylphenidate. *Journal of Child Psychology and Psychiatry*, *52*(7), 761–771. doi:10.1111/J.1469-7610.2010.02333.X.

Lin, A. L., Poteet, E., Du, F., Gourav, R. C., Liu, R., Wen, Y., et al. (2012). Methylene blue as a cerebral metabolic and hemodynamic enhancer. *PloS One*, *7*(10), e46585. doi:10.1371/journal.pone.0046585.

Maldjian, J. A., Laurienti, P. J., Kraft, R. A., & Burdette, J. H. (2003). An automated method for neuroanatomic and cytoarchitectonic atlas-based interrogation of fMRI data sets. *NeuroImage*, *19*(3), 1233–1239. doi:10.1016/s1053-8119(03)00169-1.

Markett, S., Reuter, M., Montag, C., Voigt, G., Lachmann, B., Rudorf, S., et al. (2014). Assessing the function of the fronto-parietal attention network: insights from resting-state fMRI and the attentional network test. *Human Brain Mapping*, *35*(4), 1700–1709. doi:10.1002/hbm.22285.

Martinez, J. L., Jensen, R. A., Vasquez, B. J., McGuinness, T., & McGaugh, J. L. (1978). Methylene-blue alters retention of inhibitory avoidance responses. *Physiological Psychology*, *6*(3), 387–390. doi:10.3758/bf03326744.

McIntosh, A. R. (2000). Towards a network theory of cognition. *Neural Networks*, *13*(8–9), 861–870. doi:10.1016/s0893-6080(00)00059-9.

McIntosh, A. R., & Gonzalez-Lima, F. (1995). Functional network interactions between parallel auditory pathways during Pavlovian conditioned inhibition. *Brain Research*, *683*(2), 228–241. doi:10.1016/0006-8993(95)00378-4.

Minzenberg, M. J., Yoon, J. H., & Carter, C. S. (2011). Modafinil modulation of the default mode network. *Psychopharmacology*, *215*(1), 23–31. doi:10.1007/S00213-010-2111-5.

Pamplona, G. S., Santos Neto, G. S., Rosset, S. R., Rogers, B. P., & Salmon, C. E. (2015). Analyzing the association between functional connectivity of the brain and intellectual performance. *Frontiers in Human Neuroscience*, *9*, 61. doi:10.3389/fnhum.2015.00061.

Pankevich, D. E., Altevogt, B. M., Dunlop, J., Gage, F. H., & Hyman, S. E. (2014). Improving and accelerating drug development for nervous system disorders. *Neuron*, *84*(3), 546–553. doi:10.1016/j.neuron.2014.10.007.

Peter, C., Hongwan, D., Kupfer, A., & Lauterburg, B. H. (2000). Pharmacokinetics and organ distribution of intravenous and oral methylene blue. *European Journal of Clinical Pharmacology*, *56*(3), 247–250. doi:10.1007/s002280000124.

Raichle, M. E. (2015). The Brain's default mode network. *Annual Review of Neuroscience*, *38*, 433–447. doi:10.1146/annurev-neuro-071013-014030.

Riha, P. D., Rojas, J. C., & Gonzalez-Lima, F. (2011). Beneficial network effects of methylene blue in an amnestic model. *NeuroImage*, *54*(4), 2623–2634. doi:10.1016/j.neuroimage.2010.11.023.

Rodriguez, P., Jiang, Z., Huang, S., Shen, Q., & Duong, T. Q. (2014). Methylene blue treatment delays progression of perfusion-diffusion mismatch to infarct in permanent ischemic stroke. *Brain Research*, *1588*, 144–149.

Rojas, J. C., Bruchey, A. K., & Gonzalez-Lima, F. (2012). Neurometabolic mechanisms for memory enhancement and neuroprotection of methylene blue. *Progress in Neurobiology*, *96*(1), 32–45. doi:10.1016/j.pneurobio.2011.10.007.

Scheindlin, S. (2008). Something old... something blue. Molecular Interventions, 8(6), 268–273, doi:10.1124/mi.8.6.1.

Scott, A., & Hunter Jr., F. E. (1966). Support of thyroxine-induced swelling of liver mitochondria by generation of high energy intermediates at any one of three sites in electron transport. *The Journal of Biological Chemistry*, *241*(5), 1060–1066.

Shen, Q., Du, F., Huang, S., Rodriguez, P., Watts, L. T., & Duong, T. Q. (2013). Neuroprotective efficacy of methylene blue in ischemic

stroke: an MRI study. *PloS One*, *8*(11), e79833. doi:10.1371/journal.pone.0079833.

Shirer, W. R., Ryali, S., Rykhlevskaia, E., Menon, V., & Greicius, M. D. (2012). Decoding subject-driven cognitive states with whole-brain connectivity patterns. *Cerebral Cortex*, *22*(1), 158–165. doi:10.1093/Cercor/Bhr099.

Telch, M. J., Bruchey, A. K., Rosenfield, D., Cobb, A. R., Smits, J., Pahl, S., et al. (2014). Effects of post-session administration of methylene blue on fear extinction and contextual memory in adults with claustrophobia. *The American Journal of Psychiatry*, *171*(10), 1091–1098. doi:10.1176/appi.ajp.2014.13101407.

Tzourio-Mazoyer, N., Landeau, B., Papathanassiou, D., Crivello, F., Etard, O., Delcroix, N., et al. (2002). Automated anatomical labeling of activations in SPM using a macroscopic anatomical parcellation of the MNI MRI single-subject brain. *NeuroImage*, *15*(1), 273–289. doi:10.1006/nimg.2001.0978.

Walter-Sack, I., Rengelshausen, J., Oberwittler, H., Burhenne, J., Mueller, O., Meissner, P., et al. (2009). High absolute bioavailability of methylene blue given as an aqueous oral formulation. *European Journal of Clinical Pharmacology*, *65*(2), 179–189. doi:10.1007/s00228-008-0563-x.

Wang, Z., Aguirre, G. K., Rao, H., Wang, J., Fernandez-Seara, M. A., Childress, A. R., et al. (2008). Empirical optimization of ASL data analysis using an ASL data processing toolbox: ASLtbx. *Magnetic Resonance Imaging*, *26*(2), 261–269. doi:10.1016/j.mri.2007.07.003.

Watts, L. T., Long, J. A., Chemello, J., Van Koughnet, S., Fernandez, A., Huang, S., et al. (2014). Methylene blue is neuroprotective against mild traumatic brain injury. *Journal of Neurotrauma*, *31*(11), 1063–1071. doi:10.1089/neu.2013.3193.

Watts, L. T., Long, J. A., Boggs, R. C., Manga, H., Huang, S., Shen, Q., et al. (2015). Delayed methylene blue improves lesion volume, multi-parametric quantitative magnetic resonance imaging measurements, and behavioral outcome after traumatic brain injury. *Journal of Neurotrauma*. doi:10.1089/neu.2015.3904.

Whitfield-Gabrieli, S., & Nieto-Castanon, A. (2012). Conn: a functional connectivity toolbox for correlated and anticorrelated brain networks. *Brain Connectivity*, *2*(3), 125–141. doi:10.1089/brain.2012.0073.

Witt, S. T., Laird, A. R., & Meyerand, M. E. (2008). Functional neuroimaging correlates of finger-tapping task variations: an ALE meta-analysis. *NeuroImage*, *42*(1), 343–356. doi:10.1016/j.neuroimage.2008.04.025.

Wrubel, K. M., Riha, P. D., Maldonado, M. A., McCollum, D., & Gonzalez-Lima, F. (2007). The brain metabolic enhancer methylene blue improves discrimination learning in rats. *Pharmacology, Biochemistry, and Behavior*, *86*(4), 712–717. doi:10.1016/J.Pbb.2007.02.018.

Zhang, X., Rojas, J. C., & Gonzalez-Lima, F. (2006). Methylene blue prevents neurodegeneration caused by rotenone in the retina. *Neurotoxicity Research*, *9*(1), 47–57. doi:10.1007/bf03033307.